Colloidal Au Catalyst Preparation: Selective Removal of Polyvinylpyrrolidone from Active Au Sites

Baira Donoeva* and Petra E. de Jongh*[a]

Colloids with controlled dimensions, morphology and composition can be used to obtain supported metal catalysts with desired characteristics. Yet, removal of capping agents which block active metal sites in such catalysts can be challenging: mild methods often result in incomplete removal of capping agents, whereas harsher methods can cause change in particle size or morphology or cause metal segregation for bimetallic particles. Here we provide evidence that polyvinylpyrrolidone used as a stabilizing agent for gold colloids is present both on the metal and the support surface after colloid deposition on the TiO$_2$ support. The polymer adsorbed on Au sites blocks their catalytic activity if it cannot be desorbed/decomposed under reaction conditions. Polyvinylpyrrolidone can be removed completely from the active gold surface of Au/TiO$_2$ without particle growth using a number of mild treatment methods described in this work, despite only partial removal ($\approx 45\%$) of the stabilizer from the bulk of Au/TiO$_2$ can be achieved. The remaining $> 50\%$ of polyvinylpyrrolidone resides exclusively on the TiO$_2$ support and has no effect on the optical properties and catalytic activity of gold nanoparticles. The treated catalysts demonstrate catalytic activity and selectivity similar to those of a catalyst prepared by impregnation. These findings are important for further advancing the preparation of well-defined supported catalysts using metal colloids.

Introduction

Metal colloids are widely used in catalysis research owing to the possibility to precisely control their size, composition, nanostructure, and morphology.[1] This precise control could allow one to establish the relationship between catalyst structure/composition and its properties, thus providing a basis for the rational design of more active, selective and stable catalysts. Typically, metal colloids are synthesized in solution in the presence of an excess of stabilizing (capping) agents/ligands or surfactants, such as amines, thiols, phosphines, polymers, etc. which control the size/shape of forming nanoparticles and protect them from aggregation.[1] An excess of the stabilizing agent is typically used to efficiently stabilize metal nanoparticles. Colloids are subsequently deposited on the surface of a support material to obtain heterogeneous catalysts. Free molecules of the stabilizing agent that are present in colloidal solution in excess with respect to the metal can potentially bind to the support surface along with the capped nanoparticles. For example, a recent study showed indications that the majority of polyvinylalcohol (PVA), used as a stabilizing agent for Pd nanoparticles, was present on the surface of the carbon support and only a minor fraction of it was in direct contact with Pd nanoparticles.[2] Therefore it can be hypothesized that a supported catalyst prepared from polymer stabilized colloidal nanoparticles can be schematically depicted as shown in Figure 1.

Although stabilizing agents can be used to tune catalyst activity or selectivity,[3] the presence of the ligands on the metal surface after immobilization of colloids on the support more often becomes detrimental for catalysis because they (partially) block active metal sites. Additionally, the presence of stabiliz-
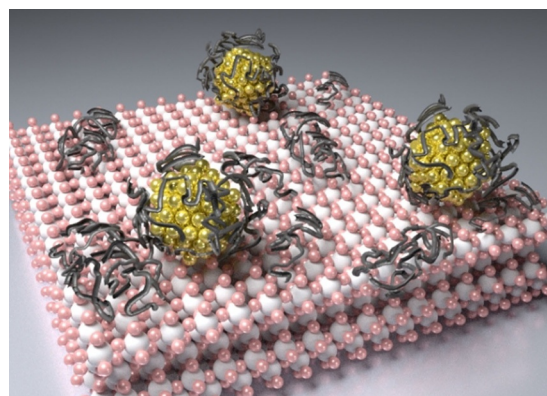
[a] Dr. B. Donoeva, Prof. P. E. de Jongh
Inorganic Chemistry and Catalysis,
Debye Institute for Nanomaterials Science
Utrecht University
Universiteitweg 99, 3584 Utrecht (The Netherlands)
E-mail: b.donoeva@uu.nl
        p.e.dejongh@uu.nl

Figure 1. A proposed schematic representation of untreated polymer-stabilized metal nanoparticles immobilized on a catalyst support (e.g. Au-PVP/TiO$_2$). Polymer-capped nanoparticles are present on the support together with polymer not bound to metal nanoparticles.

ing agents on the surface of metal nanoparticles brings complexity into the interpretation of catalytic results owing to the unknown effect of the stabilizers on reactant/product adsorption, ligand–metal charge transfers, stability, etc.[3c] Therefore, removal of capping agents from metal nanoparticles without affecting their size and structure is an important aspect of catalyst preparation using colloidal particles. Strategies that are commonly used to remove capping agents from supported metal nanoparticles can be divided into three main categories: decomposition of the stabilizer using high temperature, UV light or ozone; solvo(thermal) treatments to extract ligands with the excess of solvent; or treatment with small molecules to displace bulky stabilizing agents.[3c, 4]

Polyvinylpyrrolidone (PVP) is one of the most commonly used stabilizing agents for colloidal metal nanoparticles. It can also serve as a shape-directing and reducing agent.[5] PVP binds to the surface of metal nanoparticles through carbonyl groups and/or the nitrogen atom of the pyrrolidone ring.[6] Removing PVP from metal nanoparticles has proven to be difficult: the high temperature treatment ($>300\,°C$) under oxidizing conditions required to decompose PVP often leads to changes in the particle size or morphology.[7] Moreover, incomplete PVP decomposition leads to the formation of coke, which poisons the catalyst.[4a]

Recently, several promising mild methods for the removal of PVP from different metal nanoparticles >6 nm have been reported, such as treatment with $NaBH_4$ or *tert*-butylamine;[8] however these methods were demonstrated only for unsupported large colloids, and thus their efficiency for smaller and support-immobilized metal nanoparticles has not been established yet. In some cases, it was suggested that PVP could be removed by subjecting a catalyst to reaction conditions. For example, Albonetti et al. suggested partial PVP removal from Au nanoparticles supported on ceria during the oxidation of 5-hydroxymethylfurfural (HMF) in water at $70\,°C$ by PVP displacement with HMF molecules.[9] However neither the wider applicability, nor the efficiency of this approach are yet clear.

Capping agents that are weakly adsorbed on the metal surface, for example, do not form covalent bonds with metal centers, and can in principle be removed by washing with an excess of a solvent that interacts well with the molecules of the capping agent, given that enough time/heat is provided. Polyvinyl alcohol (PVA) was partially removed from TiO_2-supported Au nanoparticles by extracting them with water at $90\,°C$.[4b] The mean size of Au nanoparticles increased from 3.0 to 4.4 nm (3-fold increase in the particle volume) as $\approx 20\%$ (wt.%) of the overall PVA was removed from Au/TiO_2. The removal of PVA from gold nanoparticles resulted in an increase in the catalytic activity for the oxidation of CO, benzyl alcohol and glycerol.

Since Haruta's discovery of the exceptional catalytic activity of gold nanoparticles in the low temperature oxidation of carbon monoxide,[10] the catalytic properties of gold have been actively investigated in various reactions.[11] The high catalytic activity of small Au particles (≈ 2 nm) often originates from their high surface-to-volume ratio and specific nanoscale effects, such as altered structural and electronic properties, as

well as interaction with the support.[12] Preparation of small supported gold nanoparticles is not always trivial for some supports using traditional deposition-precipitation or impregnation methods. Therefore immobilization of pre-formed gold nanocolloids is often employed to obtain excellent control over the particle size and morphology independently of the support chosen.[13] Removal of stabilizing agents from small nanoparticles <3 nm can be especially challenging since they often grow during ligand removal.[4b]

The main aim of the current work is to systematically investigate promising methods, reported previously for other systems, to efficiently remove PVP from 2–3 nm TiO_2-immobilized gold nanoparticles and achieve maximum PVP removal with minimum change in Au particle size or the catalyst gold loading. Special attention was paid to whether PVP was removed from the active gold surface, support surface or both; and whether complete PVP removal from the active gold surface can be achieved. Our results indicate that PVP can be removed quantitatively from the active surface of gold nanoparticles despite incomplete PVP removal from the TiO_2 support, and the catalytic activity of such treated catalysts is similar to that of catalysts with the same particles prepared using the impregnation method.

Results and Discussion

Figure 2 shows representative TEM images and the corresponding particle size distributions of PVP-stabilized Au colloid synthesized in methanol and Au/TiO_2 prepared from this colloid. As seen from Figure 2, gold nanoparticles were successfully immobilized on TiO_2 without any change in the particle size during the deposition step. ICP analysis showed that gold loading of the Au/TiO_2 was 0.92 wt.%, close to the target value of 1 wt.% (Table 1, entry 1). This Au/TiO_2 catalyst (referred to as
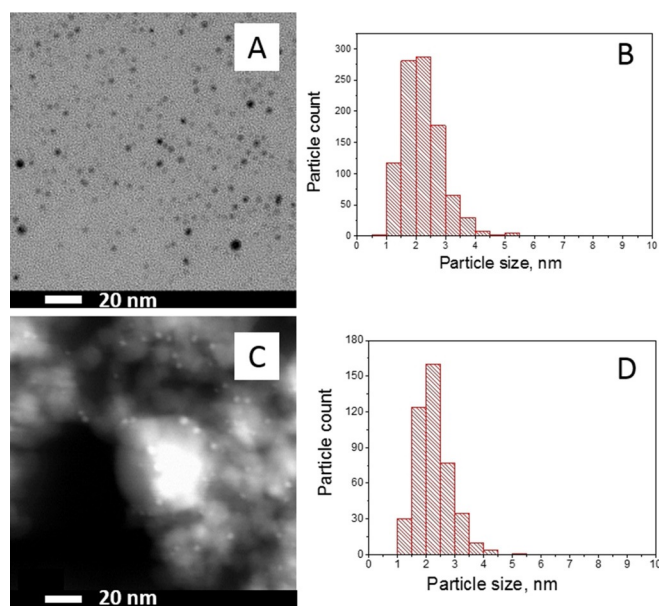

Figure 2. Representative TEM images and corresponding particle size distributions of Au-PVP colloids (A and B) and untreated Au/TiO_2 (C and D).

Table 1. Au loadings in untreated and treated Au/TiO$_2$ and the extent of PVP removal determined by different techniques.

	Catalyst/Treatment	Au loading [wt %][a]	PVP content [wt %][b]	PVP removed [wt %][b]	PVP removed [wt %][c]
1	Au/TiO$_2$ untreated	0.92	1.79	–	–
2	Au/TiO$_2$_BHx1	0.92	1.64	8	12
3	Au/TiO$_2$_BHx5	0.90	0.97	46	16
4	Au/TiO$_2$_H$_2$O	0.81	0.80	55	n.d.
5	Au/TiO$_2$_BH, H$_2$O	0.88	1.33	26	15
6	Au/TiO$_2$_TBA	0.89	1.28	29	n.d.
7	Au/TiO$_2$_BH/TBA	0.84	1.09	39	n.d.

[a] Determined from ICP. [b] Determined from TGA. [c] determined from XPS.

untreated) was used as the starting material to investigate the influence of a series of treatments on the removal of PVP from the 2–3 nm gold nanoparticles.

Extent of PVP removal during liquid-phase treatments

We first investigated the effect of six mild treatments (RT) on the overall PVP and gold content in Au/TiO$_2$ catalysts: treatment with either NaBH$_4$, H$_2$O, *tert*-butylamine (TBA), as well as some of their combinations (see Experimental Section for details). Both NaBH$_4$ and TBA are expected to displace PVP from gold nanoparticles, whereas water treatment is expected to desorb PVP from the catalyst as a result of PVP solvation with water molecules.[15]

Figure 3 shows the results of thermogravimetric analysis of the bare TiO$_2$ support and Au/TiO$_2$ catalysts before and after treatments. For clarity, only the temperature range of 250–600 °C in which PVP decomposition takes place is provided (See Figures S1 and S2 for more details). In this temperature range, two phenomena are responsible for the weight loss: decomposition of PVP at 350 °C and desorption of residual strongly adsorbed water from TiO$_2$ surface.
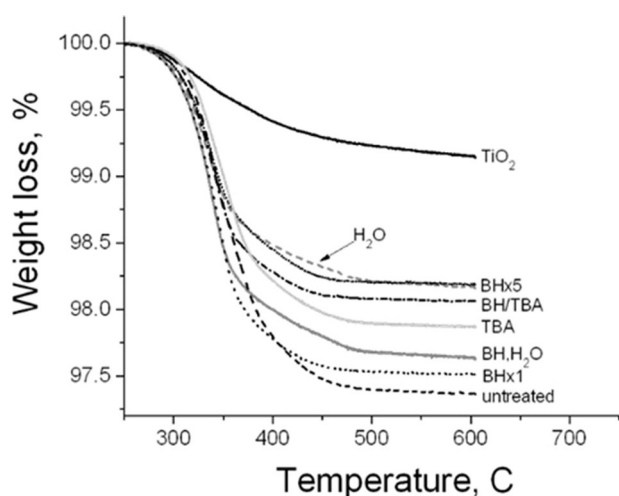

Figure 3. Thermogravimetric analysis of bare TiO$_2$, untreated Au/TiO$_2$ and Au/TiO$_2$ treated using different methods. Except for TiO$_2$, only the treatment codes are provided in Figure.

An overview of the PVP content in the Au/TiO$_2$ sample series quantified from the TGA results is given in Table 1. Untreated Au/TiO$_2$ contained 1.79 wt.% of PVP, the highest content within the series (Table 1, Figure 3). All treated catalysts show reduced content of PVP compared to the untreated sample, however neither of the treatments led to the complete removal of the stabilizer. As seen from Table 1, the efficiency of NaBH$_4$ treatment increases with the number of repetitions (Table 1, entries 2, 3) and presence of NaBH$_4$ is crucial, as washing with the solvent (methanol) alone did not lead to any change in the PVP content in Au/TiO$_2$ (not shown).

ICP characterization (Table 1) showed that Au loading was reduced during the H$_2$O and BH/TBA treatments, indicating leaching of Au nanoparticles from the TiO$_2$ support (Table 1, entry 4). No metal leaching was observed for any other of the investigated treatments. Interestingly, during consecutive treatments with NaBH$_4$ and H$_2$O (Au/TiO$_2$_BH,H$_2$O) the PVP content was reduced from 1.79 to 1.33 wt.% (26% PVP loss) with almost no decrease in the Au loading (cf. H$_2$O treatment, Table 1, entries 4, 5) which could be a result of the direct contact between the TiO$_2$ support and the nanoparticles that is induced by the NaBH$_4$ treatment.

Thus, all six tested treatments resulted in the partial removal of PVP from Au/TiO$_2$ catalysts, and the repeated treatment with NaBH$_4$ and single H$_2$O wash showed the highest efficiencies. Treatments with H$_2$O and a combination of NaBH$_4$ and TBA also caused leaching of 9–12% of gold from the catalysts, and therefore these treatments have been excluded from further studies.

From where is the PVP removed?

Methods such as TGA show the exact PVP content in the bulk Au/TiO$_2$, and it is possible to quantify the precise fraction of PVP removed from the bulk catalyst after treatments, as it was shown in the previous section. However it is not possible to distinguish whether it is TiO$_2$- or Au-bound PVP that was removed during the treatments (see Figure 1). For most applications, such as catalysis, only the removal of the capping agent from the surface of the active phase (gold) is of interest.

TGA results show that not all of the PVP is removed from the bulk Au/TiO$_2$ during the studied treatments, therefore we further investigated whether the remaining PVP resided on the Au particles or on the TiO$_2$ support.

High-resolution N 1s and Au 4f X-ray photoelectron spectra of the untreated Au/TiO$_2$ and Au/TiO$_2$_BH,H$_2$O are shown in Figure 4. Table 2 gives an overview of the relative nitrogen and gold contents in selected Au/TiO$_2$ catalysts quantified from N 1s and Au 4f peaks, respectively. In all cases, the amount of nitrogen-containing species was reduced by 11–16% upon treatment, which agrees with the removal of PVP. Table 1 shows the percentage of PVP removed calculated from XPS.

Furthermore, the gold content determined from XPS increased by 25–33% during the treatments. This increase in Au content after treatments can be explained by the surface
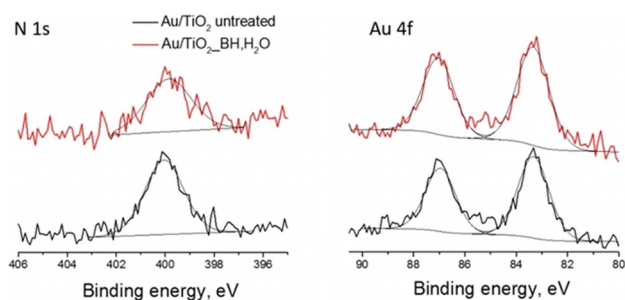
Figure 4. High-resolution N 1S and Au 4f spectra of the untreated Au/TiO$_2$ and Au/TiO$_2$_BH,H$_2$O.

Table 2. XPS characterization of untreated and treated Au/TiO$_2$.					
Sample	Element	Peak area	RSF [a]	Normalized peak area	area$_{element}$/area$_{Ti}$
Au/TiO$_2$ untreated	Au 4f	1201	17.1	70.2	0.012
	N 1s	714	1.8	396.4	0.068
	Ti 2p	45 373	7.8	5809.7	
Au/TiO$_2$_BH,H$_2$O	Au 4f	1046	17.1	61.2	0.016
	N 1s	399	1.8	221.9	0.058
	Ti 2p	29 861	7.8	3823.4	
Au/TiO$_2$_BHx1	Au 4f	1114	17.1	65.2	0.015
	N 1s	481	1.8	266.9	0.060
	Ti 2p	34 426	7.8	4407.9	
Au/TiO$_2$_BHx5	Au 4f	1421	17.1	83.1	0.015
	N 1s	560	1.8	311.3	0.057
	Ti 2p	42 640	7.8	5459.7	
[a] Relative sensitivity factor for XPS transitions from Casa XPS.					

nature of the XPS technique. That is, in the untreated Au/TiO$_2$ gold nanoparticles are partially blocked by the PVP shell, therefore a fraction of gold is not detected. After PVP removal more gold is detected because the bare surface of Au nanoparticles is exposed. Thus, XPS gives an indication that PVP is removed directly from the surface of Au nanoparticles during the studied treatments.

Ultraviolet-visible spectroscopy is another technique that can be used to directly trace changes in the surrounding environment of plasmonic Au nanoparticles, such as ligand removal, because the position and intensity of the localized surface plasmon resonance (LSPR) band of metal nanoparticles are highly sensitive to the surrounding environment. Figure 5 shows diffuse-reflectance (DR) UV-Vis spectra of the untreated and treated Au/TiO$_2$ catalysts. All spectra possess a pronounced band centered at ≈ 520 nm corresponding to the LSPR of Au nanoparticles. An intense LSPR band of the untreated Au/TiO$_2$ is centered at 526 nm. Upon a single treatment with NaBH$_4$ the LSPR band shifted to 518 nm and its intensity decreased considerably.

The color of the catalyst after the treatment was appreciably different (Figure S3). Considering that the size of Au particles does not change, as seen from TEM characterization (see below), and DR UV-Vis spectrum of pure TiO$_2$ support does not change upon NaBH$_4$ treatment (Figure S4), we conclude that the observed change in the optical properties of Au/TiO$_2$ is a

result of the removal of PVP from the surface of Au nanoparticles. The observed blue shift of the SPR position is also in agreement with the theoretical prediction. Both the position and the intensity of the SPR band are proportional to the dielectric constant of the surrounding medium according to the Drude model and Mie theory.[16,17] Dielectric constants of air (STP), PVP and methanol are 1.00, 2.31 and 1.74, respectively. Therefore, in the case of PVP removal from Au nanoparticles, the position of the LSPR band should shift to lower wavelengths and the LSPR band intensity should decrease, which is observed experimentally. A similar trend in the LSPR band position shift was also observed for unsupported 10-nm Au nanoparticles upon NaBH$_4$ treatment.[8a] Thus DR UV-Vis provides another confirmation that PVP is removed directly from the surface of gold nanoparticles.

Further treatments of Au/TiO$_2$_BHx1 with NaBH$_4$ (Au/TiO$_2$_BHx5) or H$_2$O (Au/TiO$_2$_BH,H$_2$O) caused only minor decrease in the LSPR band intensity and no change in the band position, despite their substantially lower PVP content compared to Au/TiO$_2$_BHx1 as seen from TGA results (Table 1). The spectra of Au/TiO$_2$_BHx5 and Au/TiO$_2$_BH,H$_2$O were identical. This indicates that only minor changes in the surrounding of Au nanoparticles in Au/TiO$_2$_BHx1 occur during subsequent NaBH$_4$ or H$_2$O treatments. This could be owing to the fact that a single treatment with an excess of NaBH$_4$ already removes most of the PVP from the Au surface since BH$_4^-$ binds strongly and more selectively to the Au surface (67 kcal mol^{-1}),[8a] thus displacing most of the adsorbed PVP. Subsequent treatments with NaBH$_4$ or H$_2$O remove the remains of the PVP bound to Au nanoparticles as well as free PVP molecules from the TiO$_2$ support. Removal of most of the PVP from gold nanoparticles upon single treatment with NaBH$_4$ can also explain the absence of gold leaching upon the subsequent H$_2$O treatment for Au/TiO$_2$_BH,H$_2$O, since Au nanoparticles are no longer capped with PVP, therefore their solubility in a certain solvent is not determined by the solubility of PVP. In-
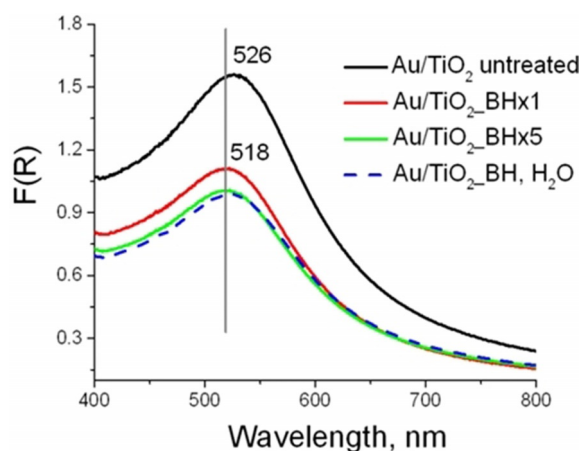
Figure 5. Diffuse-reflectance UV-vis spectra of Au/TiO$_2$ before and after selected treatments. Vertical grey line is given as a guide for the eye.

complete removal of PVP upon a single treatment with $NaBH_4$ contrasts with treatment of unsupported colloidal Au particles, for which addition of an excess of $NaBH_4$ caused quantitative PVP desorption.[8a] Therefore the presence of a support material reduces the efficiency of PVP desorption from Au by treatment with $NaBH_4$.

TGA results show a significant discrepancy in the PVP content in Au/TiO_2_BHx5 and $Au/TiO_2\_BH,H_2O$ (0.97 and 1.33 wt.%, respectively), however DR UV-Vis spectra of the two catalysts are identical. This indicates that in both cases PVP is completely removed from the gold nanoparticles, whereas the difference in the PVP content in Au/TiO_2_BHx5 and $Au/TiO_2\_BH,H_2O$ is a result of the difference in the amount of TiO_2-bound PVP, which has no effect on the Au LSPR band position and intensity.

Impact of the treatments on Au particle size

Figure 6 shows representative TEM images of treated Au/TiO_2 catalysts. There was no change in the size and size distribution of supported gold nanoparticles upon treatments with $NaBH_4$, and $NaBH_4$ followed by H_2O. However, during TBA treatment the size of Au particles increased to 3.4 nm, which corresponds to a ca. 3-fold increase in the particle volume on average (Fig-

ure 6C), therefore the TBA treated Au/TiO_2 was also excluded from the subsequent catalytic testing.

Catalytic activity: Oxidation of 5-hydroxymethylfurfural and benzyl alcohol

For a given Au particle size, the catalytic activity is proportional to the number of the active sites accessible to reactants. Considering that Au particle size does not change during selected treatments, measurement of the catalytic activity of treated and untreated Au/TiO_2 can be used as a probe for the number of available active sites, and hence indirectly show the extent of removal of the stabilizing agent from gold nanoparticles. For example, Quintanilla et al. demonstrated that the activity of the reference Au/Al_2O_3 catalyst, supplied by the World Gold Council and prepared by deposition precipitation, in benzyl alcohol oxidation decreased 6–8 times after the catalyst was subjected to a treatment with an excess of dodecylamine (DDA) and PVP capping agents.[18] This reduction in activity was ascribed to the poisoning/blocking effect of these capping agents. Recyclability tests of the PVP- and dodecylamine-"poisoned" Au catalysts showed slight improvement in the catalytic activity most likely as a result of a partial removal of the capping agent under the reaction conditions, however, the activity of DDA-capped Au catalyst even in the third cycle achieved only $\approx 40\%$ of the original activity of the capping agent-free reference catalyst (80 °C, solvent: toluene, 1 atm air).

We investigated the activity of a series of Au/TiO_2 catalysts in two representative reactions: oxidation of 5-hydroxymethyl-furfural (HMF) in water (Scheme 1) and oxidation of benzyl alcohol in toluene (Scheme 2). Oxidation of benzyl alcohol is often used as a reference reaction to evaluate the activity of gold catalysts.[11a] Supported gold nanoparticles were also demonstrated to be efficient catalysts in the oxidation of HMF to 2,5-furandicarboxylic acid (FDCA), an important transformation for the production of bio-based polymers.[19] The oxidation of HMF proceeds via the formation of 2,5-hydroxymethylfurancarboxylic acid (HMFCA) intermediate in the presence of gold catalysts under basic conditions in water.

Table 3 summarizes the results of the catalytic testing of the untreated and treated Au/TiO_2 catalysts in the oxidation of HMF. We observed that all catalysts demonstrated the same activity in HMF conversion with TOF_{Au} of ca. 0.07 s^{-1} and similar yields of furandicarboxylic acid (FDCA) after 6 h. It should be
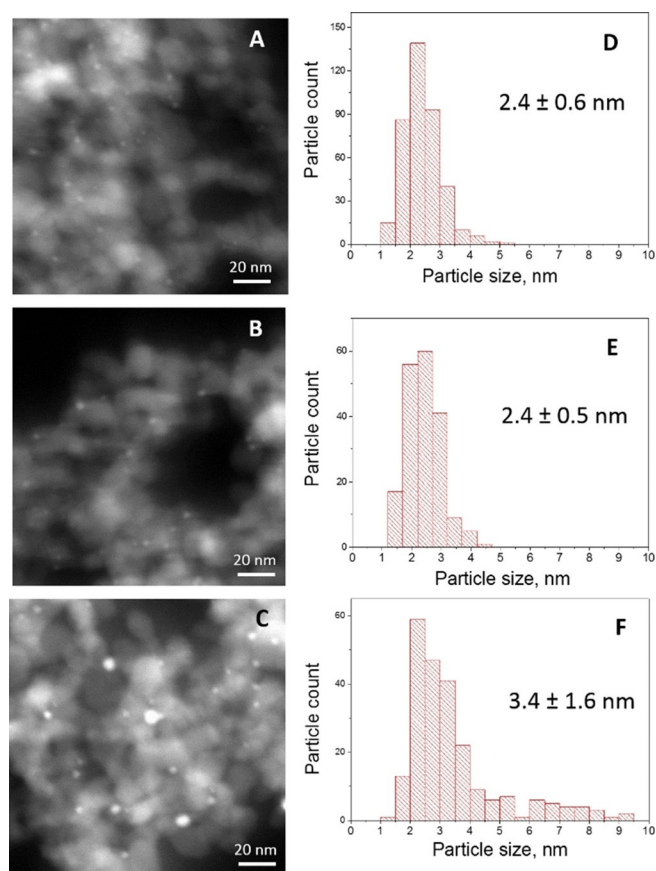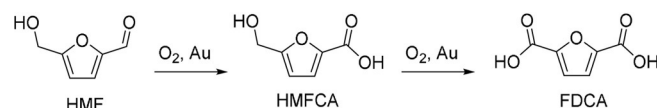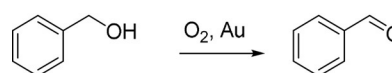

Figure 6. Representative TEM images and corresponding particle size distributions of Au/TiO_2_BHx5 (A, D), $Au/TiO_2\_BH,H_2O$ (B, E) and Au/TiO_2_TBA (C, F).

Scheme 1. Oxidation of 5-hydroxymethylfurfural (HMF) to 2,5-furandicarboxylic acid (FDCA) catalyzed by Au nanoparticles.

Scheme 2. Oxidation of benzyl alcohol.

© 2018 The Authors. Published by Wiley-VCH Verlag GmbH & Co. KGaA, Weinheim

Table 3. Oxidation of HMF over Au/TiO$_2$ catalysts.			
	Catalyst	TOF$_{Au} \times 10^{2}$ [a] [s^{-1}]	HMFCA yield [b] [%]	FDCA yield [b] [%]
1	Au/TiO$_2$_untreated	6.9	83	14
2	Au/TiO$_2$_BHx1	6.8	84	12
3	Au/TiO$_2$_BHx5	6.6	88	9
4	Au/TiO$_2$_BH,H$_2$O	6.4	89	10

Conditions: HMF 0.2 mmol, [HMF]/[Au] = 80, NaHCO$_3$ 0.4 mmol, H$_2$O 7 mL, O$_2$ 10 bar, 90 °C, 900 rpm. [a] TOF calculated as $k \cdot C^{0}/n(Au_{surf})$; where k is the rate constant obtained from linearization of kinetic curves, C^{0} is initial concentration of HMF, and $n(Au_{surf})$—number of moles of surface Au atoms. [b] Product yields are calculated after 6 h.

Table 4. Oxidation of benzyl alcohol over Au/TiO$_2$ catalysts.		
	Catalyst	TOF$_{Au}$ [s^{-1}] [a]
1	Au/TiO$_2$_untreated	0.13
2	Au/TiO$_2$_BHx1	0.28
3	Au/TiO$_2$_BHx5	0.33
4	Au/TiO$_2$_BH,H$_2$O	0.33
5	Au/TiO$_2$_imp	0.33

noted that PVP is highly soluble in water and can desorb from the Au/TiO$_2$ catalyst under aqueous conditions, as seen from the TGA results for the H$_2$O treated sample. Moreover, the high temperature of the reaction media (90 °C) strongly facilitates the process of PVP desorption.

Hence it is likely that PVP is quickly removed from the untreated Au/TiO$_2$ catalyst under the conditions of HMF oxidation (H$_2$O, 90 °C), therefore its initial presence has no effect on the catalytic activity. Similar activities of the treated and untreated catalysts also validate our conclusion that no major changes occur with the catalyst during treatment with NaBH$_4$.

The results of HMF oxidation indicate that, in this specific case, PVP can be removed by subjecting a catalyst to the reaction conditions, in line with previous suggestions.[9] However such an approach has a limited applicability for ligand removal, as it is not suitable for liquid-phase reactions in solvents in which PVP/capping agent are not soluble, as well as for gas-phase reactions at temperatures below PVP/capping agent decomposition point. For example, in the work of Quintanilla et al. it was shown that subjecting a catalyst to the reaction conditions is inefficient for PVP removal: The activity of the "poisoned" reference catalyst in the oxidation of benzyl alcohol has not been revived even after several catalytic cycles.[18] Zhao et al. performed the removal of PVA from supported Pd nanoparticles and compared their activity to that of the untreated catalysts. Authors showed that the activity of Pd nanoparticles was affected by the presence of PVA to a higher extent in the gas-phase decomposition of formic acid, than in an aqueous-phase nitrite hydrogenation.[2] Authors suggested that liquid-phase hydrogenation reaction is less sensitive to ligand presence/removal because PVA partially desorbs in the liquid-phase reaction, which does not occur in the gas-phase reaction.

Au/TiO$_2$ catalysts were also tested in the oxidation of benzyl alcohol performed in toluene. Since PVP is insoluble in toluene, PVP is not expected to quickly desorb from the gold nanoparticle surface under conditions of benzyl alcohol oxidation. Therefore the initial activity of the catalyst is expected to directly reflect the amount of accessible Au sites in the treated catalysts. Table 4 shows the results of the catalytic testing of untreated and treated Au/TiO$_2$ in the oxidation of benzyl alcohol.

Untreated Au/TiO$_2$ was active with a TOF$_{Au}$ of 0.13 s^{-1} indicating that PVP does not completely block the surface of metal nanoparticle and a fraction of the Au surface is accessible for catalysis (Table 4, entry 1). After a single treatment with an excess of NaBH$_4$ the activity of the catalyst doubled and the TOF$_{Au}$ of Au/TiO$_2$_BHx1 reached 0.29 s^{-1} (Table 4, entry 2). The TOF$_{Au}$ of Au/TiO$_2$_BHx5 and Au/TiO$_2$_BH,H$_2$O were higher and similar for both catalysts (0.33 s^{-1}, Table 4, entries 3 and 4). Since it was already shown that PVP blocks active gold sites under similar conditions,[18] the increase in the catalytic activity of Au/TiO$_2$ after NaBH$_4$ and NaBH$_4$ followed by H$_2$O treatments observed here, confirms the removal of PVP from the surface of gold nanoparticles. The results of the catalytic testing in the oxidation of benzyl alcohol correlate with DR UV-Vis results. Catalyst Au/TiO$_2$_BHx1 is less active than Au/TiO$_2$_BHx5 and Au/TiO$_2$_BH,H$_2$O owing to the presence of residual PVP, and Au/TiO$_2$_BHx5 and Au/TiO$_2$_BH,H$_2$O demonstrate similar activity and optical properties despite different bulk PVP content.

Catalyst activity is directly proportional to the number of available active metal sites for particles of the same size, hence comparison of the catalytic activity of the treated Au/TiO$_2$ with a reference catalyst that does not contain molecules of the stabilizing agent on the surface of metal particles is important. We hence prepared a Au/TiO$_2$ catalyst using a modified impregnation method (0.46 wt.%, denoted as Au/TiO$_2$_imp).[20] For TiO$_2$ as support, such method enables the obtention of small gold nanoparticles, which is not always possible with other supports. Gold nanoparticles are stabilizer-free in this catalyst as no stabilizer was involved during the synthesis. The size of Au particles was 2.4 ± 0.6 nm, similar to that of Au/TiO$_2$ prepared using colloidal gold nanoparticles, which makes the comparison more accurate as no size-dependent effects take place.

The activity of Au/TiO$_2$_imp was the same as that of Au/TiO$_2$_BHx5 and Au/TiO$_2$_BH,H$_2$O catalysts with TOF$_{Au}$ 0.33 s^{-1} (Table 4, entry 5). The same activity demonstrated by the treated Au/TiO$_2$ catalysts and stabilizer-free Au/TiO$_2$_imp strongly suggests that Au nanoparticles prepared by the colloidal route are completely free of PVP after either repeated treatment with NaBH$_4$ or NaBH$_4$ followed by H$_2$O. These results also suggest that the large amount of PVP that remains in Au/TiO$_2$ after treatments (> 50% as determined from TGA) is adsorbed on the support rather than on gold. Treatments with NaBH$_4$ and NaBH$_4$,H$_2$O therefore remove PVP more selectively from the surface of gold nanoparticles than from the TiO$_2$ support (Figure 7).

Notably, preparation of Au catalysts is not always possible using simple impregnation or deposition–precipitation meth-
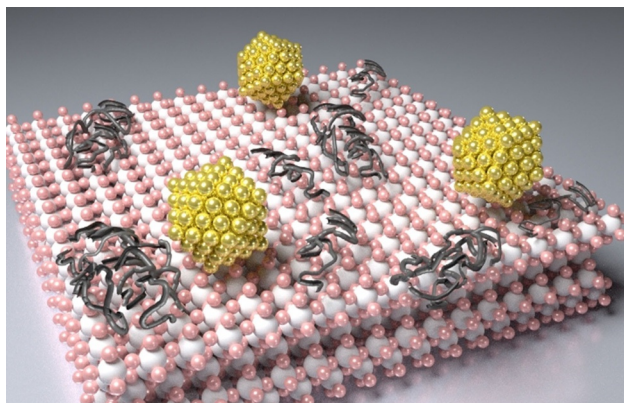
Figure 7. Schematic representation of Au/TiO$_2$ prepared by deposition of PVP-stabilized Au nanoparticles after repeated treatments with NaBH$_4$ or NaBH$_4$ followed by H$_2$O wash.

ods, for example, for acidic support materials, and therefore the colloidal method is the best alternative. Furthermore, in case that precise control over particle morphology or metal composition for bimetallic nanoparticles is required, colloidal preparation is the only suitable option. Thus, for such catalysts, the treatment methods described above can be used to efficiently remove stabilizing agents from the active surface of metal nanoparticles without affecting particle characteristics.

Conclusions

We investigated removal of PVP from 2–3 nm gold nanoparticles supported on TiO$_2$ using different ambient temperature treatments. The following conclusions can be drawn from the results of this work:

Similarly to unsupported Au colloids, NaBH$_4$ can be employed to remove PVP from supported gold nanoparticles, however owing to the presence of the support, the efficiency of the treatment is lower. That is, after a single treatment of Au/TiO$_2$ with an excess of NaBH$_4$ a small fraction of PVP still remains on the gold surface. However, both the repeated treatment of supported Au nanoparticles with an excess of NaBH$_4$, as well as consecutive treatment with a combination of NaBH$_4$ and H$_2$O remove PVP from the active surface of Au particles completely, without any change in the size of Au nanoparticles or the Au loading.

A substantial amount of PVP is still present in Au/TiO$_2$ support after the above mentioned treatments, but it resides exclusively on the TiO$_2$ support and has no effect on the catalytic activity or optical properties of the supported gold nanoparticles. This result also implies that in catalysts prepared by colloidal route the majority of stabilizing polymer ($>70\%$ in this specific case) is adsorbed on the support and not directly bound to the metal nanoparticles.

The treated Au/TiO$_2$ catalysts demonstrate catalytic performance in the oxidation of benzyl alcohol similar to that of a stabilizing agent-free catalyst prepared by impregnation, whereas the untreated Au/TiO$_2$ is 2.5 times less active. This result demonstrates that if stabilizing agent can be removed

efficiently from metal nanoparticles, the colloidal preparation method does not affect catalytic activity of the nanoparticles of similar size/structure.

Removal of a stabilizing polymer is possible by catalyst exposure to the conditions of a catalytic reaction, but only in case that the stabilizing agent is well soluble in the reaction media (liquid-phase) and does not bind strongly to the metal, or if the reaction temperature is higher than the boiling/decomposition point of a stabilizer (gas-phase). In any other case, the molecules of the stabilizer would block active sites and reduce the catalytic activity, therefore removal of a stabilizing agent is strongly advised.

This work hence provides a deeper insight into the interactions during catalyst preparation using metal colloids and demonstrates that highly active catalysts can be prepared from metal colloids if the stabilizing agent can be removed completely and without change in particle characteristics. This work also underlines the importance of specifically investigating the active sites rather than the bulk catalyst for related studies.

Experimental Section

Materials

Polyvinylpyrrolidone (PVP, MW 29000), NaBH$_4$ ($\geq$98%), HAuCl$_4$ ($>$49.0% Au), 5-hydroxymethylfurfural (HMF), 2,5-furandicarboxylic acid (FDCA), 5-hydroxymethyl-2-furancarboxylic acid (HMFCA), benzyl alcohol (99+%) and benzyl aldehyde ($>$99.0%) were purchased from Sigma Aldrich. *Tert*-butylamine (TBA), methanol (99%, extra pure) and toluene (99%+, extra pure) were purchased from Acros Organics and used without further purification. TiO$_2$ P90 (100 m^2 g^{-1}, 0.64 cm^3 g^{-1}) was purchased from Evonik.

Preparation of supported gold catalysts

PVP-stabilized Au colloids (mol [PVP]monomer/mol[Au]$=$10/1) were synthesized by adding an appropriate amount of freshly prepared solution of NaBH$_4$ (10 mg) in 5 mL of methanol (NaBH$_4$:Au$=$10:1) to a solution containing 28 mg of PVP and 10 mg of HAuCl$_4$·3 H$_2$O in 20 mL methanol at room temperature (RT). Under similar conditions larger particles are obtained in methanol compared to water, therefore 10-fold excess of PVP with respect to gold was required to efficiently stabilize small Au particles. The resulting red solution was stirred for 1 hour. Next, the obtained nanoparticles were immobilized on TiO$_2$ by adding the sol to 500 mg of the catalytic support suspended in 10 mL of methanol under vigorous stirring at RT to allow ca. 1 wt.% metal loading. After 1 h of stirring the solid was recovered by centrifugation and washed first twice with methanol and then once with diethyl ether, and subsequently dried at 60 °C overnight and at 120 °C for 2 h under static air.

Au/TiO$_2$_imp catalyst was prepared by modified incipient wetness impregnation following a procedure reported elsewhere.[20] Briefly, TiO$_2$ support was impregnated with the solution of HAuCl$_4$·3 H$_2$O (0.8 mL g^{-1} support, pH$<$1), the sample was aged at RT for 1 h then washed with aqueous ammonia solution (1 M, pH 11.5), followed by wash with deionized water and drying under vacuum at RT. Finally, the catalyst was calcined at 300 °C under static air.

PVP removal

Catalyst treatment with H_2O (treated samples denoted as Au/TiO$_2$_H$_2$O) was performed as following. Untreated Au/TiO$_2$ (500 mg) was suspended in 20 mL of deionized water (pH 6.5) and the mixture was stirred for 16 hours. The solid was then recovered by centrifugation (5000 rpm, 5 min) and washed with MeOH and diethyl ether, and dried at 60 °C.

For the treatment with NaBH$_4$, 500 mg of the catalyst was suspended in 50 mL of MeOH. NaBH$_4$ (7.5 mg) was dissolved in 20 mL MeOH at RT and added to the catalyst suspension. The mixture was kept under vigorous stirring for 2 minutes followed by catalyst recovery using centrifugation (500 rpm, 3 min), wash with MeOH and then diethyl ether, and drying at 60 °C. The sample was denoted as Au/TiO$_2$_BHx1. Other treatments consisted of either repeating this procedure 5 times in total (denoted as Au/TiO$_2$_BHx5); or consecutive treatment with NaBH$_4$×1 and H$_2$O (8 h) (denoted as Au/TiO$_2$_BH,H$_2$O).

Au/TiO$_2$ was also treated with *tert*-butylamine (denoted Au/TiO$_2$_TBA) using the following procedure: 500 mg of catalyst was suspended in 10 mL of TBA and stirred at room temperature overnight (16 h), followed by catalyst recovery by centrifugation, washing with MeOH and diethyl ether and drying at 60 °C.

Finally, treatment with a combination of NaBH4 and TBA (denoted Au/TiO2_BH/TBA) was performed by suspending 500 mg of catalyst in a solution containing 7.5 mg NaBH4 and 2 mL TBA in 18 mL of MeOH. The obtained mixture was stirred for 5 minutes at room temperature. The solid was collected by centrifugation, washed with MeOH and diethyl ether and dried at 60 °C.

Characterization

Thermogravimetric analysis (TGA) data was acquired using a PerkinElmer Pyris1TGA. Samples were heated first to 240 °C under N$_2$ flow and kept at that temperature for 1 h to remove adsorbed water, and then heated to 600 °C in a flow of 20 % of O$_2$ in N$_2$ with 10 °C min^{-1} heating rate. The PVP content in samples was calculated by subtracting the weight loss owing to H$_2$O desorption obtained for bare TiO$_2$ from the weight loss of Au/TiO$_2$ samples. For Au/TiO$_2$ subjected to aqueous wash (Au/TiO$_2$_H$_2$O and Au/TiO$_2$_BH,H$_2$O), the content of PVP was calculated as the difference of the weight loss of these Au/TiO$_2$ samples and weight loss of TiO$_2$_H$_2$O.

Gold loadings of Au/TiO$_2$ were established using inductively coupled plasma mass-spectrometry (ICP-MS) analysis. Au/TiO$_2$ samples were suspended in freshly prepared aqua regia, heated overnight, diluted with HCl solution and analyzed using ThermoFisher Scientific Element 2. Sizes of gold nanoparticles before and after treatment were established using Tecnai 12 transmission electron microscope (TEM) operating at 120 kV. Samples were suspended in ethanol, sonicated and deposited on carbon-coated Cu grids. At least 200 particles in more than 3 different spots were counted to calculate the average particle size.

Diffuse-reflectance UV-vis (DR UV-vis) spectra were recorded using a Varian Cary 500Scan UV-vis-NIR spectrophotometer equipped with an integrating sphere. Catalysts (150 mg) were loaded into a metal sample holder with a quartz window and the spectra were recorded in reflectance mode with BaSO$_4$ as a reference. The obtained reflectance values R were converted to Kubelka-Munk function F(R) using the formula: $F(R) = (1-R)^2/2R$, and the spectra were plotted as F(R) vs. λ. X-Ray photoelectron spectra were recorded at Eindhoven University of Technology, group of Prof Emiel Hensen,

using a Thermo Scientific K-Alpha spectrometer equipped with a monochromated Al$_{K\alpha}$ (hν = 1486.6 eV) X-ray source with a pass energy of 50 eV and resolution 0.1 eV. The peak binding energies were calibrated against C 1s peak at 284.5 eV. Quantitative analysis of XPS data was performed using the Casa XPS program.

Catalytic experiments

Oxidation of benzyl alcohol was performed in 12 mL stainless steel autoclaves. Typically, 25 mg of the catalyst and 1 mmol of Na$_2$CO$_3$ were suspended in 7 mL of toluene containing 0.5 mmol of benzyl alcohol and biphenyl as an internal standard. The reactor was pressurized to 10 bar with O$_2$ and the reaction was performed at 90 °C while stirring at 900 rpm. Liquid samples (100 μL) were withdrawn and analyzed by gas chromatography (GC-FID) using a Shimadzu GC-2010 equipped with a CP-WAX capillary column. Products were quantified using reference compound solutions with known concentrations.

Oxidation of 5-hydroxymethylfurfural (HMF) was performed in 12 mL stainless steel autoclaves. Typically, a catalyst (50 mg) was suspended in 7 mL of deionized water containing 0.2 mmol HMF and 0.4 mmol of NaHCO$_3$. The reactors were pressurized to 10 bar with O$_2$ and the reaction was performed at 90 °C. Samples (50 μL) were withdrawn from reaction solution and analyzed at 333 K using a high performance liquid chromatograph Shimadzu LC-20AD equipped with a refractive index detector and a Bio-Rad Aminex HPX-87H column. Sulfuric acid 5 mм in Milli-Q at a flow rate of 0.55 mL min^{-1} was used as an eluent.

TOF were calculated as $k \cdot C^0/n(Au_{surf})$; where k is the rate constant obtained from linearization of kinetic curves, C^0 is initial concentration of HMF, and $n(Au_{surf})$—number of moles of surface Au atoms; $n(Au_{surf})$ was calculated as $nAu \cdot D$, where nAu is the total number of moles of gold introduced into reaction, and D—dispersion, calculated as $6(v_m/a_m)/d_{VA}$, where v_m is volume occupied by an atom in bulk metal, a_m is area occupied by a surface atom, and d_{VA} is a mean particle size.

Conflict of interest

The authors declare no conflict of interest.

[1] a) P. Sonström, M. Bäumer, *Phys. Chem. Chem. Phys.* **2011**, *13*, 19270–19284; b) C.-J. Jia, F. Schüth, *Phys. Chem. Chem. Phys.* **2011**, *13*, 2457–2487; c) M. D. Hughes, Y.-J. Xu, P. Jenkins, P. McMorn, P. Landon, D. I.

Enache, A. F. Carley, G. A. Attard, G. J. Hutchings, F. King, E. H. Stitt, P. Johnston, K. Griffin, C. J. Kiely, *Nature* **2005**, *437*, 1132–1135; d) M. Turner, V. B. Golovko, O. P. H. Vaughan, P. Abdulkin, A. Berenguer-Murcia, M. S. Tikhov, B. F. G. Johnson, R. M. Lambert, *Nature* **2008**, *454*, 981–983.

[2] Y. Zhao, L. Jia, J. A. Medrano, J. R. H. Ross, L. Lefferts, *ACS Catal.* **2013**, *3*, 2341–2352.

[3] a) R.-Y. Zhong, K.-Q. Sun, Y.-C. Hong, B.-Q. Xu, *ACS Catal.* **2014**, *4*, 3982–3993; b) L. Tarpani, E. Mencarelli, M. Nocchetti, L. Fanò, L. Taglieri, L. Latterini, *Catal. Commun.* **2016**, *74*, 28–32; c) Z. Niu, Y. Li, *Chem. Mater.* **2014**, *26*, 72–83.

[4] a) Y. Borodko, H. S. Lee, S. H. Joo, Y. Zhang, G. Somorjai, *J. Phys. Chem. C* **2010**, *114*, 1117–1126; b) J. A. Lopez-Sanchez, N. Dimitratos, C. Hammond, G. L. Brett, L. Kesavan, S. White, P. Miedziak, R. Tiruvalam, R. L. Jenkins, A. F. Carley, D. Knight, C. J. Kiely, G. J. Hutchings, *Nat. Chem.* **2011**, *3*, 551–556; c) E. W. Elliott, R. D. Glover, J. E. Hutchison, *ACS Nano* **2015**, *9*, 3050–3059.

[5] K. M. Koczkur, S. Mourdikoudis, L. Polavarapu, S. E. Skrabalak, *Dalton Trans.* **2015**, *44*, 17883–17905.

[6] J. Xian, Q. Hua, Z. Jiang, Y. Ma, W. Huang, *Langmuir* **2012**, *28*, 6736–6741.

[7] R. M. Rioux, H. Song, M. Grass, S. Habas, K. Niesz, J. D. Hoefelmeyer, P. Yang, G. A. Somorjai, *Top. Catal.* **2006**, *39*, 167–174.

[8] a) S. M. Ansar, F. S. Ameer, W. Hu, S. Zou, C. U. Pittman, D. Zhang, *Nano Lett.* **2013**, *13*, 1226–1229; b) N. Naresh, F. G. S. Wasim, B. P. Ladewig, M. Neergat, *J. Mater. Chem. A* **2013**, *1*, 8553–8559; c) M. Luo, Y. Hong, W. Yao, C. Huang, Q. Xu, Q. Wu, *J. Mater. Chem. A* **2015**, *3*, 2770–2775.

[9] S. Albonetti, A. Lolli, V. Morandi, A. Migliori, C. Lucarelli, F. Cavani, *Appl. Catal. B* **2015**, *163*, 520–530.

[10] M. Haruta, N. Yamada, T. Kobayashi, S. Iijima, *J. Catal.* **1989**, *115*, 301–309.

[11] a) C. D. Pina, E. Falletta, M. Rossi, *Chem. Soc. Rev.* **2012**, *41*, 350–369; b) P. Claus, *Appl. Catal. A* **2005**, *291*, 222–229.

[12] a) M. Valden, X. Lai, D. W. Goodman, *Science* **1998**, *281*, 1647–1650; b) T. W. Janssens, B. Clausen, B. Hvolbæk, H. Falsig, C. Christensen, T. Bligaard, J. Nørskov, *Top Catal* **2007**, *44*, 15–26.

[13] a) F. Schüth, *Phys. Status Solidi B* **2013**, *250*, 1142–1151; b) M. Comotti, C. Weidenthaler, W.-C. Li, F. Schüth, *Top. Catal.* **2007**, *44*, 275–284; c) D. Gu, J.-C. Tseng, C. Weidenthaler, H.-J. Bongard, B. Spliethoff, W. Schmidt, F. Soulimani, B. M. Weckhuysen, F. Schüth, *J. Am. Chem. Soc.* **2016**, *138*, 9572–9580.

[14] R. Mueller, H. K. Kammler, K. Wegner, S. E. Pratsinis, *Langmuir* **2003**, *19*, 160–165.

[15] S. A. K. T. L. Lebedeva, M. M. Feldstein, and N. A. Plate in *Water Transport in Synthetic Polymers* (Eds.: O. V. S. A. L. Iordansky, G. E. Zaikov), Nova Science, New York, **2003**, pp. 69–93.

[16] P. Mulvaney, *Langmuir* **1996**, *12*, 788–800.

[17] M. Quinten, *Optical Properties of Nanoparticle Systems: Mie and Beyond*, Wiley-VCH, Weinheim, **2011**.

[18] A. Quintanilla, V. C. L. Butselaar-Orthlieb, C. Kwakernaak, W. G. Sloof, M. T. Kreutzer, F. Kapteijn, *J. Catal.* **2010**, *271*, 104–114.

[19] a) S. E. Davis, L. R. Houk, E. C. Tamargo, A. K. Datye, R. J. Davis, *Catal. Today* **2011**, *160*, 55–60; b) O. Casanova, S. Iborra, A. Corma, *ChemSusChem* **2009**, *2*, 1138–1144; c) Y. Y. Gorbanev, S. K. Klitgaard, J. M. Woodley, C. H. Christensen, A. Riisager, *ChemSusChem* **2009**, *2*, 672–675.

[20] L. Delannoy, N. El Hassan, A. Musi, N. N. Le To, J.-M. Krafft, C. Louis, *J. Phys. Chem. B* **2006**, *110*, 22471–22478.